

Prediction of RNA pseudoknots by Monte Carlo simulations

G. VERNIZZI¹, H. ORLAND¹ and A. ZEE²

¹Service de Physique Théorique, CEA/DSM/SPhT Saclay
Unité de recherche associée au CNRS
F-91191 Gif-sur-Yvette Cedex, France

²Institute of Theoretical Physics and Department of Physics
University of California, Santa Barbara, CA 93106, USA

Abstract

In this paper we consider the problem of RNA folding with pseudoknots. We use a graphical representation in which the secondary structures are described by planar diagrams. Pseudoknots are identified as non-planar diagrams. We analyze the non-planar topologies of RNA structures and propose a classification of RNA pseudoknots according to the minimal genus of the surface on which the RNA structure can be embedded. This classification provides a simple and natural way to tackle the problem of RNA folding prediction in presence of pseudoknots. Based on that approach, we describe a Monte Carlo algorithm for the prediction of pseudoknots in an RNA molecule.

arXiv:q-bio/0405014v1 [q-bio.BM] 19 May 2004

1 Introduction

In recent years the quest for an algorithm which can predict the spatial structure of an RNA molecule given its chemical sequence has received considerable attention from molecular biologists [1]. In fact the three-dimensional structure of an RNA molecule is intimately connected to its specific biological function in the cell (e.g. for protein synthesis and transport, catalysis, chromosome replication and regulation) [2]. It is determined by the sequence of nucleotides along the sugar-phosphate backbone of the RNA. The chemical formula or sequence of covalently linked nucleotides along the molecule from the 5' to the 3' end is called the *primary structure*. The four basic types of nucleotides are adenine (A), cytosine (C), guanine (G) and uracil (U), but it is known that modified bases may appear [3].

At high enough temperatures, or under high-denaturant conditions RNA molecules have the three-dimensional structure of a free single-stranded swollen polymer. At room temperature, different nucleotides can pair by means of saturating hydrogen bonds. The standard Watson-Crick pairs are A•U and C•G with two and three hydrogen bonds respectively, whereas G•U is a wobble pair with two hydrogen bonds. Comparative methods showed that “non-canonical” pairings are also possible [4], as well as higher-order interactions such as triplets, or quartets. In this paper we will consider only canonical base-pair interactions. Adjacent base pairs can stack, providing an additional binding energy which is actually the origin of the formation of stable A-form helices, one of the main structural characteristics of folded RNAs. Helices may embed unpaired sections of RNA, in the form of hairpins, loops and bulges. It is all these pairings, stackings of bases and structural motifs which bring the RNA into its folded three-dimensional configuration. One of the main open problems of molecular biology is the prediction of the actual spatial molecular structure of RNA (i.e. its *shape*) given its primary structure.

As we shall see in Section 2, it is possible to define *secondary structures* of RNA as structures in which the pairings between canonical base pairs do not cross in a certain representation (planar graphs). One can also define the *tertiary structure* of RNA which is the actual three-dimensional arrangement of the base sequence. This classification corresponds to the fact that the secondary structure of RNA carries the main contribution to the free energy of a fully folded RNA configuration, including also some of the sterical constraints. For that reason one can attempt to describe the folding process hierarchically [2, 5, 6, 7]. However, since the secondary structure describes just the topology of binary contacts of the bases, most of the information about distances in real three-dimensional space is lost. The importance of the secondary structure relies in the fact that it may provide the “skeleton” of the final tertiary structure.

Over the past twenty years several algorithms have been proposed for the prediction of RNA folding. They are based on: deterministic or stochastic minimization of a free energy function [8, 9], phylogenetic comparison [10, 11, 12, 13], kinetic folding [14, 15, 16, 17], maximal weighted matching method [18], and several others (for a survey see [19]). It is fair to say that despite the large number of tools available for the prediction of RNA structures, no reliable algorithms exist for the prediction of the full tertiary structure of RNA. Most of the algorithms listed above deal with the prediction of just the RNA secondary structure. To describe the full folding it is important to introduce the concept of RNA pseudoknot [20]. One says that two base pairs form a pseudoknot when the parts of the RNA sequence spanned by those two base pairs are neither disjoint, nor have one contained in the other. Thus RNA secondary structures without pseudoknots can be represented by planar diagrams, whereas RNA with pseudoknots appear when two base pairs can “cross”, leading to non-planar diagrams (a more precise definition is given in the next Section). Pseudoknots play an important role in natural RNAs [21], for structural, regulatory and catalytic functions. Pseudoknots are excluded in the definition of RNA secondary structure and many authors consider them as part of the tertiary structure. This restriction is due to the fact that RNA secondary structures without pseudoknots

can be predicted easily. One should also note that pseudoknots very often involve base-pairing from distant parts of the RNA, and are thus quite sensitive to the ionic strength of the solution. It has been shown that the number of pseudoknots depends on the concentration of Mg^{++} ion, and can be strongly suppressed by decreasing the ionic strength (thus enhancing electrostatic repulsion) [22, 23, 24]. The most popular and successful technique for predicting secondary structures is dynamic programming [8, 25, 26, 27, 28, 29, 30, 31], for which the memory and CPU requirements scale with the sequence length L as $O(L^2)$ and $O(L^3)$, respectively.

Recently, new deterministic algorithms that deal with pseudoknots have been formulated [32, 33, 34, 35, 36, 37, 38, 39, 40]. In this case the memory and CPU requirements generally scale as $O(L^4)$ and $O(L^6)$ respectively ($O(L^4)$ and $O(L^5)$ in [35], or $O(L^4)$ and $O(L^3)$ for a restricted model in [34]), which can be a very demanding computational effort even for short RNA sequences ($L \sim 100$). Moreover, the main limitation of these algorithms is the lack of precise experimental informations about the contribution of pseudoknots to the RNA free energy, which is often excluded a priori in the data analysis (as also pointed out in [16, 41, 42]). The increase of computational complexity does not come as a surprise. In fact the RNA-folding problem with pseudoknots has been proven to be NP-complete for some classes of pseudoknots [34, 35]. For that reason, stochastic algorithms might be a better choice to predict secondary structures with pseudoknots in a reasonable time and for long enough sequences.

In [9, 43, 44, 45] stochastic Monte Carlo algorithms for the prediction of RNA pseudoknots have been proposed. In these stochastic approaches, the very irregular structure of the energy landscape (glassy-like) is the main obstacle: configurations with small differences in energy may be separated by high energy barriers, and the system may very easily get trapped in metastable states. Among the stochastic methods, the direct simulation of the RNA-folding dynamics (including pseudoknots) with kinetic folding algorithms [16, 17] is most successful. This technique allows to describe the succession of secondary structures with pseudoknots during the folding process. The approach we follow in this paper is close in spirit to that one, with a stronger emphasis on the topological character of the RNA pseudoknots. It is based on a correspondence (first noticed by E. Rivas and S.R. Eddy in [32]) between a graphical representation of RNA secondary structures with pseudoknots and Feynman diagrams. In [32] the authors consider only a particular class of pseudoknots. Along the same direction, the authors of [38] made the correspondence between RNA folding and Feynman diagrams more explicit by formulating a *matrix field theory* model whose Feynman diagrams give exactly all the RNA secondary structures with pseudoknots. The remarkable facts of this new approach is that it provides an analytic tool for the prediction of pseudoknots, and all the diagrams appear to be naturally organized in a series of terms, called the *topological expansion*, where the first term corresponds to planar secondary structures without pseudoknots, and higher-order terms correspond to structures with pseudoknots.

In this paper we explore in more detail this topological expansion and its potential predictive power. We also propose a numerical stochastic algorithm for dealing with this expansion in a systematic way, which in principle allows the prediction of all kinds of RNA pseudoknots. The paper is organized as follows. In Section 2 we review some well-known graphical representation of RNA structures, with special emphasis on the so-called “disk diagram” representation. In such a representation one can uniquely associate to each RNA secondary structure with (or without) pseudoknots, a circle diagram which is planar (or not planar, respectively). In Section 3 we show how one can characterize the “degree of non-planarity” of a given disk diagram. In fact, one can always associate an integer number to each RNA disk diagram, called the *genus*, and we will describe its topological meaning and information content. We thus propose to classify RNA pseudoknots according to their genus. Following this idea, in Section 4 we generalize the standard thermodynamic model for the description of RNA structures to the inclusion of pseudoknots. The generalized model we propose is very natural, in the same spirit when going from the Canonical Ensemble to the Grand Canonical Ensemble in statistical mechanics.

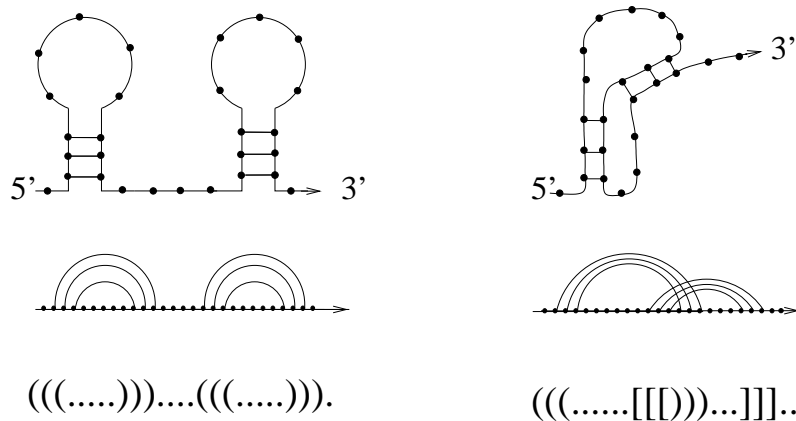


Figure 1: An RNA configuration without pseudoknots (left column) and RNA configuration with a simple “H” pseudoknot (right column). From the top to the bottom: the RNA configuration, arc representation and bracket representation. Note that the arc diagram for pseudoknotted RNA has crossing arcs and the bracket representation requires two kinds of parenthesis.

Our model can control the topological fluctuations i.e. the formation of pseudoknots in the RNA molecule, and we will describe the general features of its phase diagram. In Section 5 we describe a Monte Carlo algorithm for the actual calculation of thermodynamical quantities in our generalized model. In particular we will list in details the Monte Carlo moves, the free-energy updating algorithm and the simulated annealing method we propose for dealing with the problem of high energy barriers. Section 6 contains the concluding remarks, and the Appendix is devoted to the explicit description of a part of the Monte Carlo algorithm of Section 5.

2 Representation of RNA structures

Any RNA sequence can be represented as the list of nucleotides $r_i \in (A, C, G, U)$, $i = 1, \dots, L$, where r_i is the i -th nucleotide along the oriented sugar backbone (from 5' to 3'). The ordered list $\{r_1, r_2, \dots, r_L\}$ is called the primary structure of the RNA.

The RNA secondary structure requires a more graphical representation. Actually there are several equivalent ways to represent an RNA secondary structure with a given primary structure. The most commonly used representation is perhaps the *bracket* notation, where two paired bases, r_i and r_j ($i < j$), are represented by parenthesis “(“ and “)”, and unpaired bases are represented by a dot ‘.’ or a colon ‘:’ (see Figure 1). Pseudoknots can be described in a similar fashion, but one needs to introduce several different kinds of brackets (like square brackets ‘[’, ‘]’ or braces ‘{’, ‘}’, as for example in the database [46, 47]), and this is not a very efficient representation for complicated structures.

Among several other representations (e.g. mountain diagrams [48], tree diagrams [49], graphs [50]), a very general and widely used representation is the so-called *dot plot* diagram. It is an array where a dot is placed in the row i and column j if the bases r_i and r_j are actually paired (see Figure 2). This plot is the graphical representation of the $L \times L$ *contact matrix* C with elements

$$C_{ij} = \begin{cases} 1 & \text{if } i \text{ and } j \text{ are paired,} \\ 0 & \text{otherwise.} \end{cases} \quad (2.1)$$

In mathematical terms, the contact matrix C is the matrix of the permutation involution associated to the given set of pairings. In fact, one can always interpret the base pairing $i - j$ as a transposition

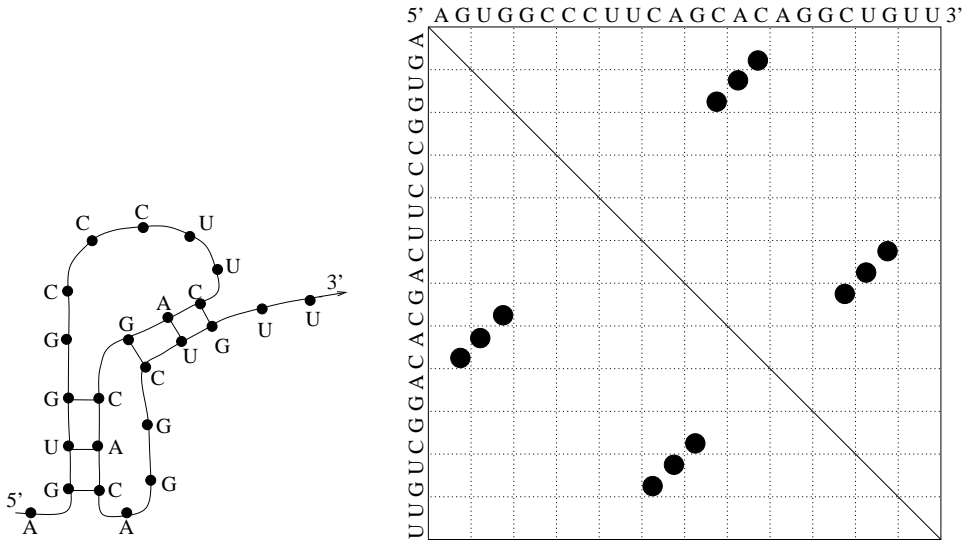


Figure 2: Representation of an RNA secondary structure with an “H” pseudoknot (left), and the corresponding dot plot diagram (right).

of the elements $\{i, j\}$ and therefore one can uniquely associate a permutation σ to any structure by:

$$\sigma(i) = \begin{cases} j & \text{if } i \text{ and } j \text{ are paired,} \\ i & \text{otherwise.} \end{cases} \quad (2.2)$$

For example, if the primary structure is $\{5' - CUUCAUCAGGAAAUGAC - 3'\}$ and the pseudoknotted secondary structure is: $.(((.[[[])]..]))$, one can associate to it the permutation:

$$\sigma = \begin{pmatrix} . & (& (& (& . & [& [& [&) &) &) & . & . &] &] &] & . \\ 1 & 2 & 3 & 4 & 5 & 6 & 7 & 8 & 9 & 10 & 11 & 12 & 13 & 14 & 15 & 16 & 17 \\ 1 & 11 & 10 & 9 & 5 & 16 & 15 & 14 & 4 & 3 & 2 & 12 & 13 & 8 & 7 & 6 & 17 \end{pmatrix}, \quad (2.3)$$

which is also an involution since σ^2 is the identity permutation. The matrix representation of σ is the matrix D with $D_{i,\sigma(i)} = 1$ and 0 otherwise. Obviously $D = C + \mathcal{I}$, where \mathcal{I} is the $L \times L$ identity matrix. This notation is very useful for numerical implementations of the algorithm we propose in Section 5. The advantage of the dot plot diagram is that it allows the comparison between different RNA secondary structures, just by superimposition as it is necessary for comparative analysis. Moreover it can be used for representing RNA structure with any kind of pseudoknots.

A representation which is completely equivalent to the dot plot diagram is the *disk diagram* (also called *circle plot* or *circular plot*). In this case the RNA sequence is represented as an oriented circle (from 5' to 3') by virtually linking the first nucleotide to the last one. Each base pairing is represented as an arc inside the circle, connecting the two paired bases. Figure 3 shows a typical disk diagram. In this representation secondary structures without pseudoknots are purely planar diagrams, i.e. diagrams that can be drawn without crossing arcs, whereas pseudoknots correspond to structures which are not planar. This fact has been already observed by E.Rivas and S.R.Eddy in [32], where they consider diagrams with arcs inside *and* outside the disk¹. Crossing arcs are allowed but only inside or only outside but not both at the same time (so-called “overlapping pseudoknots”, see diagrams a) and b) of Figure 4). As it was shown in [39, 40], several general classes of pseudoknots

¹More precisely, they represent the RNA sequence as an oriented straight line, and the pairings as arcs above and below that line. This is of course equivalent to the disk representation.

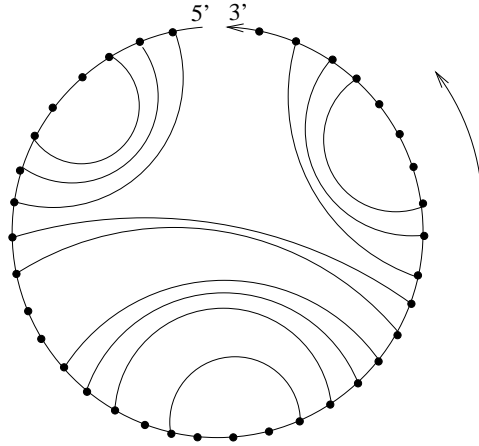


Figure 3: Typical disk (circle) diagram representation of an RNA secondary structure without pseudoknots. The circle is anticlockwise oriented from 5' to 3'. Note that there are no crossing arcs.

cannot be described in such a simple way (such as the diagram on the right of Figure 4). It is then more convenient to draw the arcs always inside the disk (or outside, but not both) and to consider all the corresponding diagrams as non planar. It is precisely following this approach that the authors of [38] found an algorithm for computing pseudoknots with matrix field theory in a completely general fashion. In this paper we pursue the same analysis by considering the diagrams themselves and not the associated matrix field theory model.

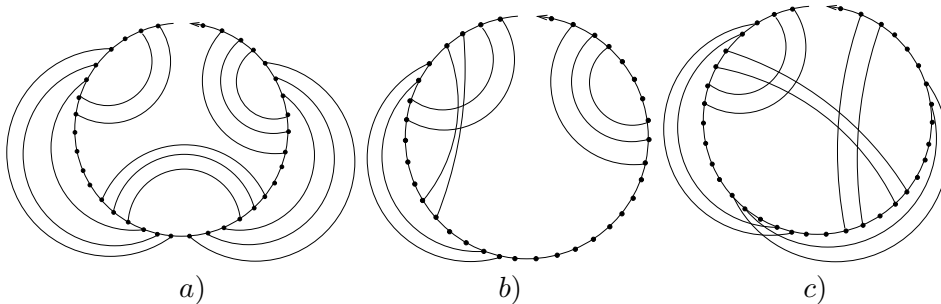


Figure 4: Three kind of disk diagrams for RNA secondary structures with pseudoknots. The authors of [32] consider cases of the form a) (“overlapping pseudoknots”), b) (pseudoknot present in *Escherichia coli* α mRNA [51]) but not c) (parallel β -sheet protein interaction). The technique in [38] can deal with all the three cases.

3 The topological character of RNA pseudoknots

There is a very natural way for classifying the “degree of non-planarity” of a given disk diagram, which we review here briefly. It is based on a topological analysis introduced long ago by Euler. We emphasize that this characterization is a well-known classical result of algebraic topology and it has been already introduced in [38] for RNA secondary structures. We repeat it here in more detail for the convenience of the reader.

As we have shown, in any disk diagram the RNA sequence is represented by an oriented circle. When the circle is drawn on a sphere, its orientation allows to distinguish an “inside” and an “outside”

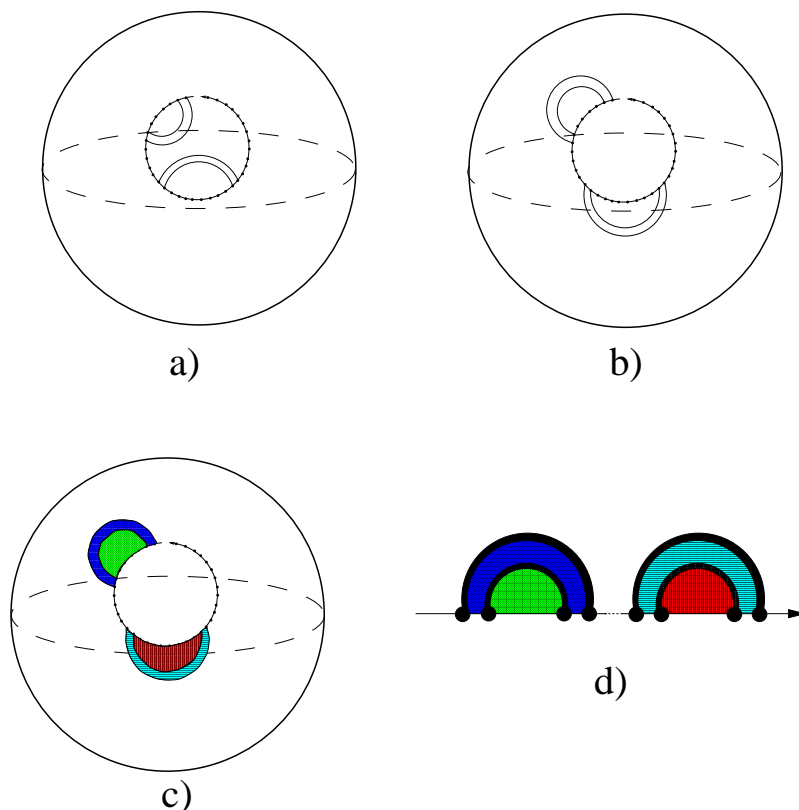


Figure 5: Example of planar disk diagram. In a) the disk diagram of a double hairpin (like the one in Figure 1) is on a sphere. In b) the arcs are drawn all outside the circle. In c) the sphere is partitioned in 6 patches (5 faces and one “hole”, i.e. the RNA circle). In d) is the representation of c) in double line notation (black thick arcs). Here $\#F = 5$, $\#V = 4$, $\#E = 8$, and therefore $\chi = 1$, i.e. $g = 0$.

of the circle. One says that the circle is a “boundary” or “puncture” (as it can be drawn smaller and smaller, in a continuous fashion up to single point) on the sphere. Hence any (disk) planar diagram can be drawn on a sphere without crossing lines, simply by drawing the arcs on the same side (see Figure 5). The key observation is that the sphere is naturally partitioned in several parts by the diagram. As explained in [38] it is useful to draw the arcs with a “double-line notation” (see Figure 5). In this way it is clear that the sphere is partitioned into several polygons. Note that all the lines have an orientation induced by the one of the circle.

The Euler characteristic χ of a diagram is defined as

$$\chi = \#V - \#E + \#F, \quad (3.1)$$

where $\#V$, $\#E$ and $\#F$ are the numbers of vertices, edges, and faces, respectively. A vertex is just a nucleotide, an edge is any line connecting two nucleotides (either an arc joining the nucleotides, or the RNA sequence) and a face is that part of the surface within a closed loop of edges. Obviously, if there are n arcs then $\#E = \#V + n$. A famous theorem of Euler states that any polyhedron homeomorphic to a sphere with a boundary (puncture) has an Euler characteristic $\chi = 1$. Therefore all RNA secondary structures without pseudoknots are described by disk diagrams with $\chi = 1$.

Let us discuss the case when there is a pseudoknot. For simplicity, we consider a “kissing hairpin” pseudoknot. In this case the corresponding disk diagram is not planar, and has crossing arcs (see for instance Figure 6). After drawing the disk diagram in double line notation, and counting the number

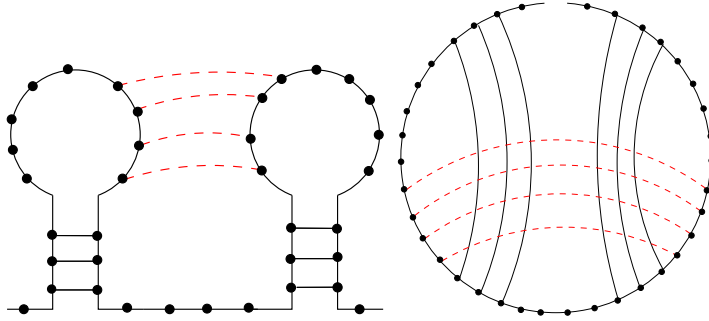


Figure 6: A “kissing hairpin” pseudoknot. The respective disk diagram has crossing arcs necessarily, when the arcs are drawn all inside (or all outside) the RNA circle.

of vertices, edges and faces, one gets that $\chi = -1$ this time. This value has a precise geometrical meaning. In fact, the Euler characteristic of a surface (or of a manifold in general) is closely related to its *genus* g , i.e. the number of “handles” of the surface. Namely if the manifold is orientable (as the disk diagram is, since the oriented circle line defines naturally an orientation of all the elements of the diagram), then one has $\chi = 2 - 2g - c$ where c is the number of punctures ($c = 1$ in the case we consider here, with only one RNA strand). It follows that a kissing hairpin is represented by a disk diagram with genus $g = 1$. One concludes then, that such a disk diagram can be drawn on an oriented manifold with one handle, that is a *torus* (which is a doughnut-shaped surface formed by taking a cylinder and joining the two circular ends together, see Figure 7). This procedure can be extended easily to cases with more complex pseudoknots. For instance, the three diagrams of Figure 4 have genus $g = 2$, $g = 1$ and $g = 2$, respectively. In Figure 8 there is a graphical representation of all 8 types of irreducible pseudoknots with genus $g = 1$ (from [39]) and in Figure 9 there is some examples of pseudoknots with a higher genus.

Thus we have a simple way to classify pseudoknots. This classification corresponds exactly to the series expansion of the partition function of the matrix model proposed in [38]. There, the series is in powers of the form N^{-2g} , where N is the size of the matrix, and g is the genus of the corresponding set of diagrams. In the next section, we will exploit the same idea and show how one can control the topological character of pseudoknots in a statistical mechanical model for RNA secondary structures with pseudoknots.

4 Statistical mechanics model of RNA structures with pseudoknots

In almost all the energy models for RNA which have been proposed in recent years, the thermodynamical properties of a single stranded RNA are studied by means of a partition function of the form

$$\begin{aligned}
 \mathcal{Z}_{RNA} &= \int \prod_{k=1}^L d\mathbf{r}_k \sum_{C_{ij}} f(\{\mathbf{r}\}) e^{-\frac{1}{k_B T} U(C_{ij}, \{\mathbf{r}\})} \sim \sum_{C_{ij}} \omega(C) e^{-\frac{1}{k_B T} E(C)} = \\
 &= \sum_{C_{ij}} e^{-\frac{1}{k_B T} [E(C) - TS(T, C)]}, \tag{4.1}
 \end{aligned}$$

where T is the temperature, k_B is the Boltzmann constant, \mathbf{r}_k is the three-dimensional position vector of the k -th nucleotide, $f(\{\mathbf{r}\})$ takes into account the geometry and the constraints of the chain of

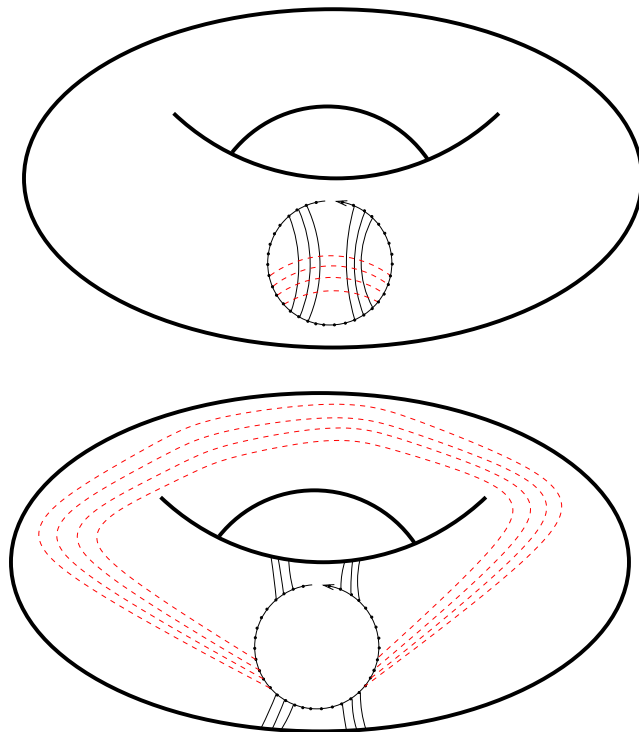


Figure 7: The “kissing hairpins” of Figure 6 can be drawn on a torus without intersections. In this example $\#F = 9$, $\#V = 20$, $\#E = 20 + 10$, and therefore $\chi = -1$, i.e. $g = 1$.

nucleotides, the function U takes into account the energetics coming from the pairing and stacking of base pairs, and the sum over C_{ij} is the sum over all possible contact matrices for a given primary structure. The function $\omega(C)$ is proportional to the number of configurations having the same contact matrix C , and therefore its logarithm is just the entropy factor associated to the polymeric nature of the sugar-phosphate backbone. The free energy of a given configuration $\mathcal{F}(C) \equiv E(C) - TS(T, C)$ is the sum of several contributions, both of energetic ($E(C)$) and entropic nature ($S(C)$): Watson-Crick and wobble base pairs, stacking energies, terminal mismatches and dangling energies, special triloops and tetraloops, entropy contributions (internal loops, bulges, hairpin loops), penalty factors for terminal-AU in helices, for asymmetries etc. All these terms have been determined empirically, and they are called “Turner energy rules” [52]. For more details see [53]. When pseudoknots are excluded, the sum in eq. (4.1) is restricted over contact matrices that correspond to planar diagrams only. As we mentioned already in the introduction, the partition function \mathcal{Z}_{RNA} without pseudoknots can be calculated efficiently by deterministic algorithms (dynamic programming) [54]: the most popular ones are perhaps the “mfold package” by M.Zuker et al. [55, 56] and the “RNA Vienna package” by I.Hofacker et al. [57]². When pseudoknots are included, the sum in eq. (4.1) is unrestricted and, as we described in the previous Section, this leads to topology fluctuations. This situation is very common also in other areas of Physics (e.g. dynamical triangulations [58], random surfaces or quantum gravity [59], quantum field theory [60]), and there are now standard ways to deal with it. The idea is to introduce an additional parameter μ , which is a topological “chemical potential”, and to consider the partition function:

$$\mathcal{Z}_{RNA}(\mu) = \sum_{C_{ij}} e^{-\frac{1}{k_B T} [E(C) - TS(T, C) + \mu g(C)]}, \quad (4.2)$$

²They are available on-line at www.bioinfo.rpi.edu/applications/mfold/ and www.tbi.univie.ac.at/, respectively.

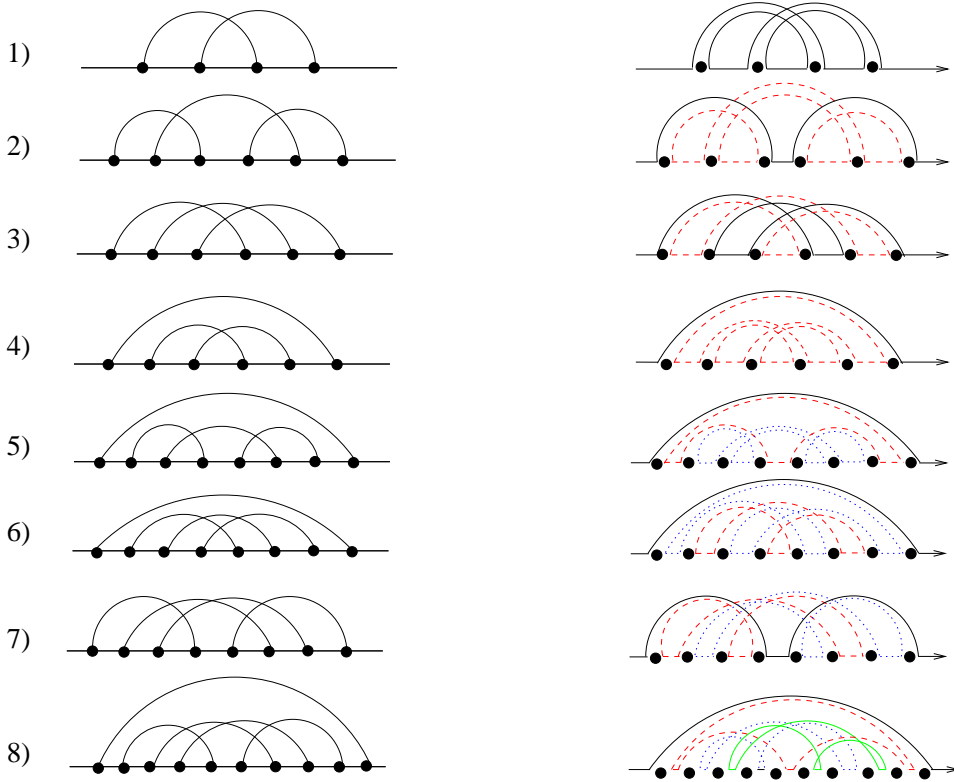


Figure 8: List of all eight irreducible diagrams with genus $g = 1$ (from [40]) and their representation with double line notation, on the left column and right column, respectively.

where $g(C)$ is the genus of the configuration associated to the contact matrix C . The “chemical potential” μ allows a simple control over the topological character of the pseudoknots in the statistical ensemble at thermal equilibrium. It is also directly related to N (the size of the matrix) in the matrix model formulation of [38]:

$$\mathcal{Z}_{Matrix} \sim 1 + \frac{Z_1}{N^2} + \frac{Z_2}{N^4} + \dots,$$

with $\mu = -2k_B T \log(N)$. The advantage here is that the energy function $E(C)$ can be more realistic than the one in [38].

The model without chemical potential, i.e. $\mu = 0$, corresponds to the case where there are no restrictions on the possible fluctuations of the topology. On the other hand when μ is very large, all the configurations with $g > 0$ are suppressed by the Boltzmann weight, and in this case one recovers the planar limit (i.e. RNA secondary structures without pseudoknots). One might expect then a phase transition associated to the formation of pseudoknots. A natural order parameter is the average genus of a RNA structure with pseudoknots which can simply be recovered by taking the logarithmic derivative of the partition function

$$\langle g(\mu) \rangle = -k_B T \frac{\partial}{\partial \mu} \log \mathcal{Z}_{RNA}(\mu). \quad (4.3)$$

To our knowledge there are no available experimental data about the dependence of the genus of RNA molecules on the temperature. Informations and inputs from experiments would be highly desirable.

Figure 10 displays the expected phase diagram in the plane $\{\mu, T\}$ of our model. At high temperature, the RNA is always in a fully denaturated phase. At lower temperature and large μ the

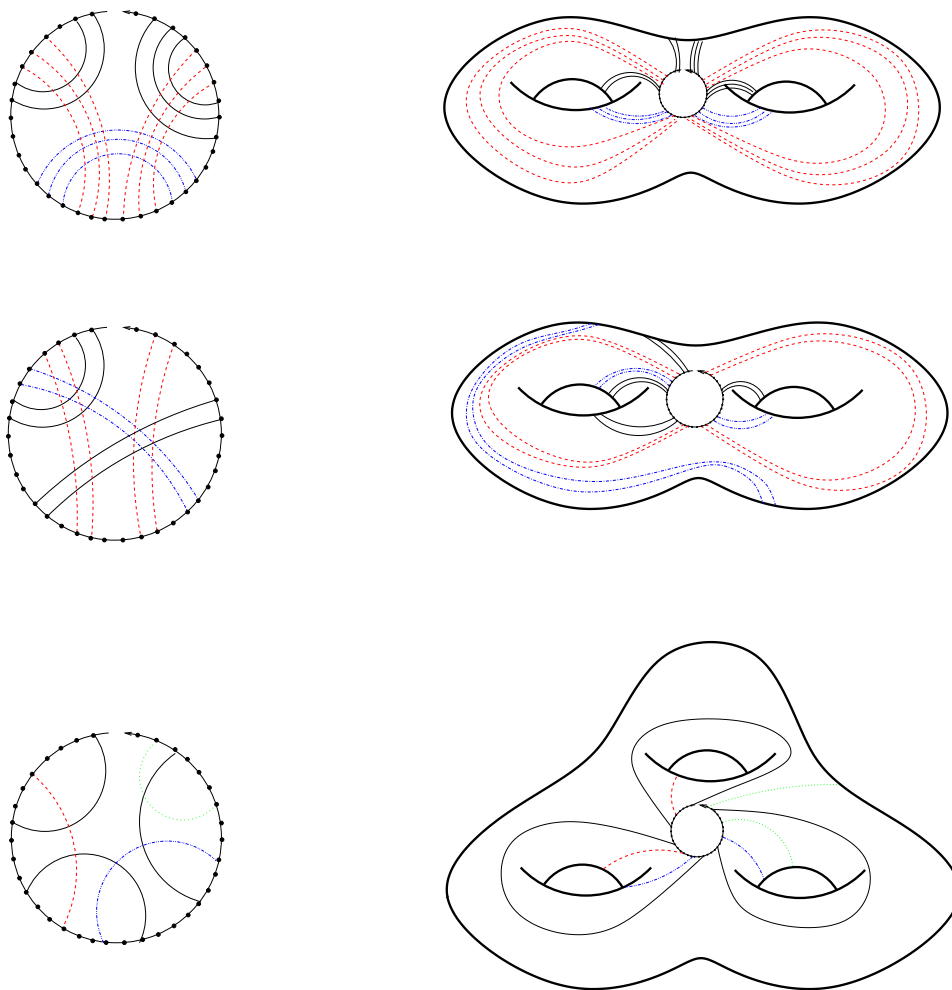


Figure 9: Example of RNA pseudoknots with higher genus. The first two plots correspond to the diagrams a) and c) of Figure 4 with genus $g = 2$. The third plot is an example with genus $g = 3$.

secondary structures without pseudoknots are the dominating configurations. The interesting part of the diagram is for lower values of μ , where possibly $\langle g(\mu) \rangle \neq 0$ and pseudoknots are present.

Even if eq. (4.2) can in principle deal with pseudoknotted RNA molecules, it is fair to say that for any realistic energy function, the model is rather unlikely amenable to an analytic solution. Moreover any dynamic programming approach has been shown to be computationally very demanding even for pseudoknots with genus $g = 1$ [40]. Hence a stochastic algorithm for studying the model eq. (4.2) is probably the only feasible way. In the next Section we describe in details a Monte Carlo algorithm for the simulation of the model of eq. (4.2).

5 A Monte Carlo algorithm for RNA pseudoknots prediction

A well-known method for generating a set of configurations which are distributed according to a given Boltzmann weight is the Monte Carlo method. It is a standard method of modern computational analysis and we refer to [61, 62] for a review and an introduction on the subject. In recent years, it has been also used for the prediction of RNA secondary structures in various contexts. In particular, our proposal can be thought of as a generalization of the Monte Carlo method described in [9] where

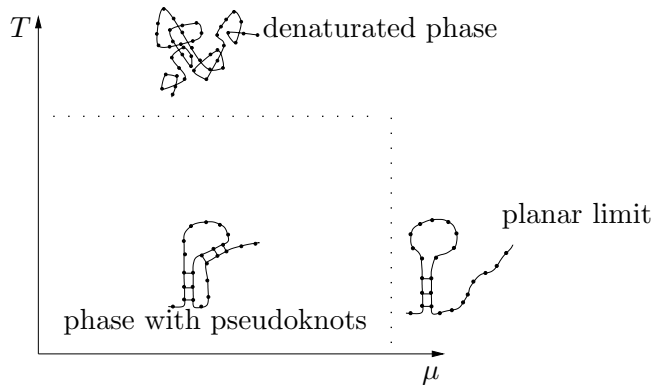


Figure 10: Qualitative structure of the phase diagram in the $\{\mu, T\}$ plane.

the authors considered only RNA secondary structures without pseudoknots. We aim to apply this method to the statistical ensemble defined by eq. (4.2).

The sum over all the RNA configurations in eq. (4.2) contains many terms. In general, the total number of RNA configurations (planar and non planar configurations) grows like $L!$ for a sequence of length L . The number of RNA configurations with a fixed genus g grows exponentially with L : a detailed analysis for the number of diagrams with genus $g = 0$ (i.e. planar diagrams) can be found in [63].³ Since the number of secondary structures on a surface with fixed genus grows exponentially, one expects that a brute force Monte Carlo importance sampling would be rather ineffective for a not too-short RNA sequence, in a reasonable amount of computation time. For that reason we decided to use the standard Metropolis method [64]. The Metropolis method is an efficient and simple scheme for generating a set of configurations distributed according to a given probability function, by means of a random walk in the configuration space. In our case, the Metropolis Monte Carlo method generates a set of n RNA configurations $\{C^{(0)}, C^{(1)}, \dots, C^{(n)}\}$, such that $\lim_{n \rightarrow \infty} n_C/n = P(C)$, where $P(C)$ is the given probability distribution (e.g., the Boltzmann distribution $P(C) = \mathcal{Z}^{-1} \exp[(E - TS + \mu g)/k_B T]$ and n_C is the number of configurations of type C in the statistical ensemble. Each element $C^{(k)}$ of the sequence is generated by accepting or rejecting a random configuration. In the following we give a complete description of the Metropolis Monte Carlo algorithm for RNA pseudoknots predictions:

- Step 1: Pick an initial configuration $C^{(0)}$: A simple initial configuration can be the fully denaturated state of RNA, i.e. the contact matrix is the matrix with all zero entries and the respective permutation involution is the identity permutation $\sigma = \begin{pmatrix} 1 & 2 & \dots & L \\ 1 & 2 & \dots & L \end{pmatrix}$. Set the variable $n = 1$.
- Step 2: Pick a trial configuration $C^{(n)}$ (by deforming the configuration $C^{(n-1)}$). Such an operation is called “Monte Carlo move” $C^{(n-1)} \rightarrow C^{(n)}$. Compute the probability ratio

$$\rho = \frac{P(C^{(n)})}{P(C^{(n-1)})}. \quad (5.1)$$

Pick a random number x with value between 0 and 1. If $x \leq \rho$ accept the configuration $C^{(n)}$ as the new configuration. Otherwise refuse it and keep $C^{(n-1)}$ as new configuration, i.e. put $C^{(n)} = C^{(n-1)}$. Increase the variable n by one.

³An analysis for structure with higher genus similar to the one in [63] is still lacking. We expect that the matrix field theory model introduced in [38] can shed some light on this issue.

- Step 3: repeat Step 2 for n_{max} times, where n_{max} is a sufficiently large number.

The most relevant aspect of this method is that, at large n_{max} , one can generate an ensemble of configurations with the probability distribution $P(C) = \mathcal{Z}^{-1} \exp[-(E(C) - TS(T, C) + \mu g(C))/(k_B T)]$, simply by computing probability ratios. Therefore, this method is extremely useful as it avoids the need of computing the partition function \mathcal{Z} of the system, a computational task that would be surely intractable for long RNA sequences.

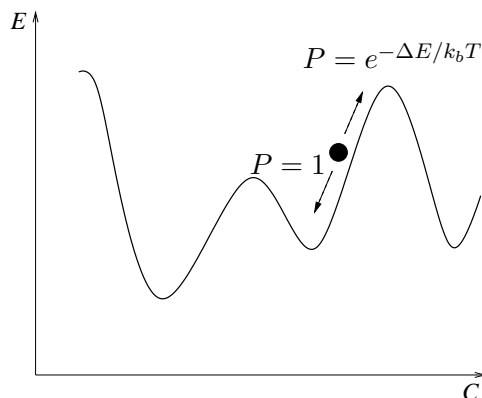


Figure 11: The Metropolis algorithm accepts a configuration with lower energy with probability $P = 1$. It can also accept a configuration with higher energy, with probability $P = e^{-\Delta E/k_b T}$, where ΔE is the energy difference.

5.1 Configurational changes (Monte Carlo moves)

At large n_{max} , the above algorithm is guaranteed to generate a set of configurations with the probability distribution $P(C)$, under few assumptions. Two essential requirements are that the Monte Carlo moves have to be *ergodic* and satisfy the so-called *detailed balance condition*. Ergodicity essentially means that every point in the configuration space can be reached in a finite number of Monte Carlo steps from any other point. The detailed balance condition here simply means that the Monte Carlo moves are symmetric, i.e. the probability of proposing a Monte Carlo move $C \rightarrow C'$ is the same as of proposing the move $C' \rightarrow C$.

We describe now the Monte Carlo moves for RNA folding. First, at the beginning of the simulation, it is useful to make some book-keeping by storing in the memory the list of all the allowed base-pairs (i.e. that are only of the type A•U, C•G or G•U). Such an information can be stored in L vectors l_i , $i = 1, \dots, L$, as follows: the nucleotide in position i can be paired to n_i possible other nucleotides, namely with the ones in position $l_i(1), l_i(2), \dots, l_i(n_i)$ and nothing else. For example, if the primary structure is $\{AGCU\}$ then we have:

$$l_1 = [4], \quad l_2 = [3, 4], \quad l_3 = [2], \quad l_4 = [1, 2]. \quad (5.2)$$

The creation of such a list of possible base-pairs does not slow down the total algorithm since it is an $O(L^2)$ operation which is done only once. Now we want to extract one element from the list of L vectors with uniform probability. This can be done as follows. Let $T \equiv \sum_h n_h$, and let pick up a uniform integer random number τ between $1 \leq \tau \leq T$. Then take the highest integer number i such that $\sum_{h=1}^i n_h \leq \tau$, and define $y \equiv \tau - \sum_{h=1}^i n_h + 1$. Obviously $1 \leq y \leq T$ holds true. Consider the pair of bases i and $j \equiv l_i(y)$. The base-pair $i - j$ has been extracted randomly with uniform probability in the set of all possible base-pairs, for the given RNA sequence. The Monte Carlo move $C \rightarrow C'$ is then generated as follows:

- If the configuration C is such that both the base in i and in j are free (i.e. $\sigma_C(i) = i$ and $\sigma_C(j) = j$) then add the link $i - j$ (i.e. put $\sigma_{C'}(i) = j$ and $\sigma_{C'}(j) = i$). We call this Monte Carlo move “add a base pair” (see case 1 of figure 12).
- If the configuration C is such that there is arc between i and j (i.e. $\sigma_C(i) = j$) then remove the link $i - j$ (i.e. put $\sigma_{C'}(i) = i$ and $\sigma_{C'}(j) = j$). We call this Monte Carlo move “remove a base pair” (see case 2 of figure 12).
- If the configuration C is such that either the base in i or the base in j is linked to some other base, (i.e. $\sigma_C(i) = i$ and $\sigma_C(j) \neq j$, or $\sigma_C(j) = j$ and $\sigma_C(i) \neq i$) then move the link back to $i - j$, by overriding any former link (i.e. put $\sigma_{C'}(i) = j$ and $\sigma_{C'}(j) = i$). We call this Monte Carlo move “shift a base pair” (see case 3 and 4 of figure 12).
- If the configuration C is such that the base i is linked to an other base k_1 and j is linked to an other base k_2 and the base-pair $k_1 - k_2$ is possible, then swap the links (i.e. put $\sigma_{C'}(i) = j$, $\sigma_{C'}(j) = i$, $\sigma_{C'}(k_1) = k_2$, $\sigma_{C'}(k_2) = k_1$). We call this Monte Carlo move “swap a base pair” (see case 5 and 6 of figure 12).
- If none of the above cases applies then do not update the configuration, i.e. put $C' = C$.

See Figure 12 for a summary of these Monte Carlo moves, and Figure 13 for a simple example.

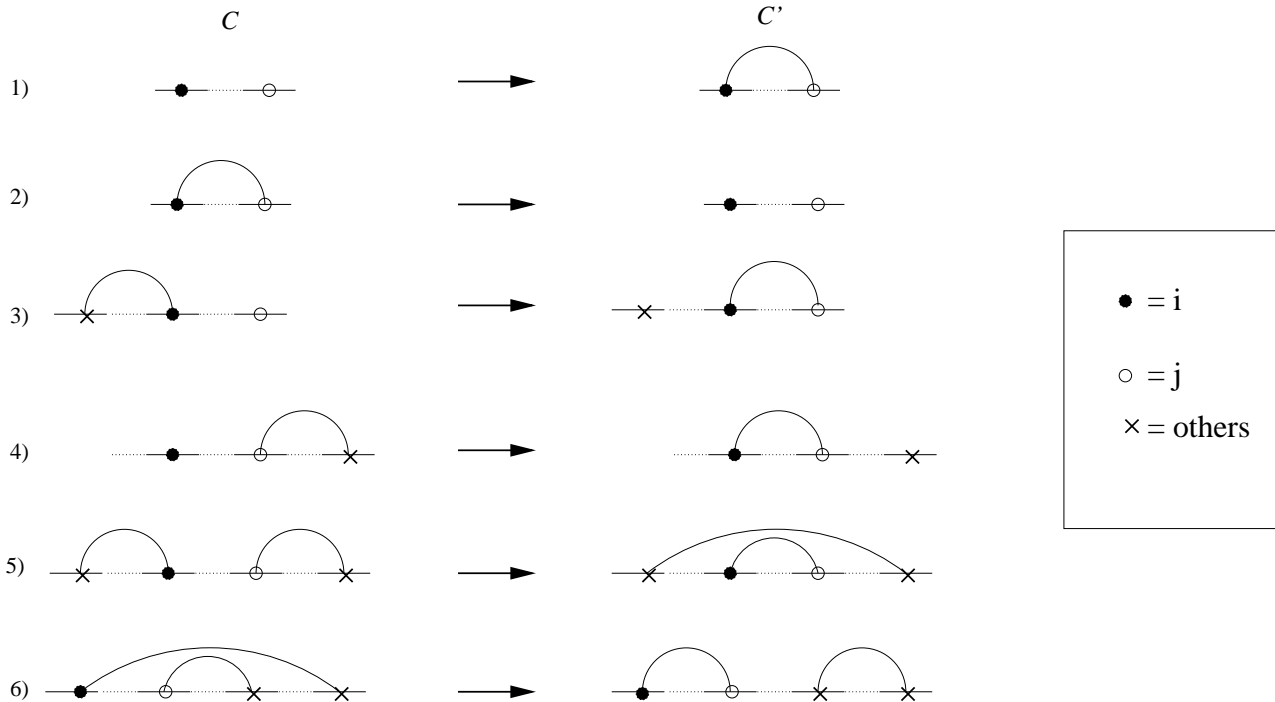


Figure 12: Monte Carlo moves for an allowed base pair $i - j$ of a RNA secondary structures with pseudoknots. The move 1) adds a base pair. The move 2) removes a base pair. The moves 3) and 4) shift a base pair. The move 5) and 6) swap two base-pairs, when possible.

These Monte Carlo moves obviously satisfy the detailed balance condition. In fact the probability of creating a link between i and j when i or j are link-free (or at least one of them), or of removing the link when they are already linked is always $P_{ij} = 2/T$, and thus it is symmetric. In the case where i

and j are already linked to different bases $\sigma(i)$ and $\sigma(j)$, then a link is put between i and j only if $\sigma(i)$ can be connected to $\sigma(j)$ as well. In this case the reverse move also occurs with the same probability rate, thus it is a symmetric move. Moreover, the set of Monte Carlo moves are ergodic. The key observation is that such moves correspond to transpositions in the space of permutation involutions. Since any configuration of RNA secondary structure with pseudoknots can be uniquely represented by a permutation involution, and since any permutation can be obtained by a suitable finite sequence of transpositions [65], it follows that any RNA secondary structure with pseudoknots can be generated with a finite number of the Monte Carlo moves described above.

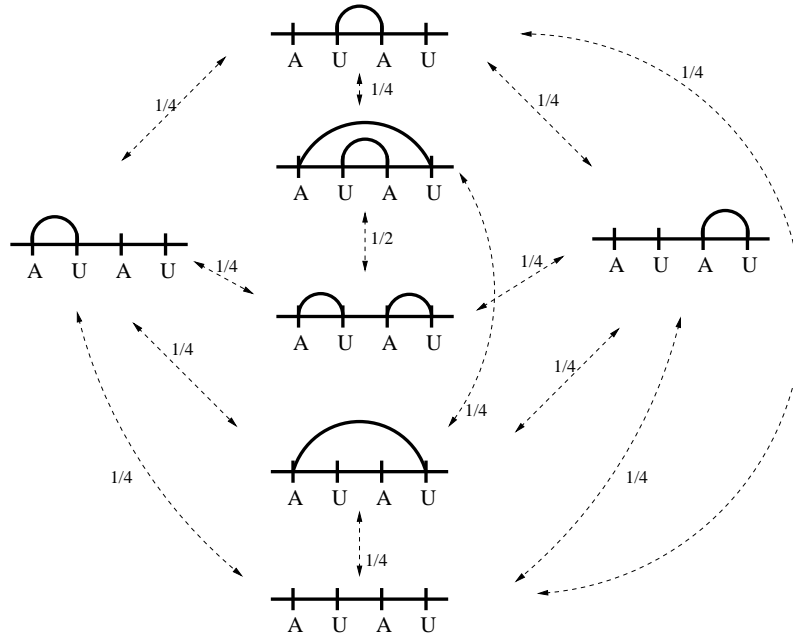


Figure 13: Space of the configurations for the sequence $\{A, U, A, U\}$. The arrows indicate the Monte Carlo moves and their probability rate.

Few comments are in order. First of all, other sets of Monte Carlo moves are possible of course. Several authors introduced collective moves, where several links are updated at the same time (as opposed to one by one as we propose). The advantages are a general speed-up of the computing time, and a more effective simulation as far as overcoming the energy barriers. In the present work, we prefer to keep the code as simple as possible by using a set of “local” moves, and to focus on testing its effectiveness when dealing with RNA pseudoknots. Second, both the generation of the Monte Carlo moves and the Metropolis method require a good (pseudo)random number generator, in order to avoid biases in the output which may be very difficult to detect. For a good introduction to random number generators we refer the reader to [66] and [67]. Finally, as in all stochastic algorithms, one has to be able to estimate the statistical errors of the Monte Carlo prediction. As this method generates an ensemble of configurations $\{C^{(0)}, C^{(1)}, \dots, C^{(n_{max})}\}$, distributed according to the probability distribution $P(C)$, then one can compute ensemble averages of any quantity $\mathcal{A}(C)$ simply by:

$$\langle \mathcal{A} \rangle = \frac{1}{n_{max}} \sum_{i=1}^{n_{max}} \mathcal{A}(C^{(i)}). \quad (5.3)$$

The error associated to this observable scales like $1/\sqrt{N}$ where N is the number of independent measurements. It is important to note that N is not usually equal to n_{max} since in general the

configurations generated by any Monte Carlo algorithm are correlated. One can deal with this issue in two ways. One can compute the autocorrelation length ξ of the sequence of the RNA configurations generated by the Monte Carlo algorithm and then subsample the same set of configurations, keeping one configuration every ξ and skipping all the configurations in between [68]. An other possibility is to keep all the configurations of the sequence, and compute the statistical error by taking into account the existence of correlations (The error is usually bigger than the simple standard deviation of the data). A well-known technique for computing the statistical error of a set of correlated data is the so-called *jackknife method*. For an introduction to this method, we refer the reader to [69]. There are also other techniques which can be found in [70].

5.2 Energy update

According to the Metropolis method, the ratio ρ (Step 2 of the algorithm, eq. (5.1)) is given by

$$\rho = \exp \left[-\frac{1}{k_B T} (\Delta E - T \Delta S + \mu \Delta g) \right], \quad (5.4)$$

where

$$\begin{aligned} \Delta E &= E(C^{(n)}) - E(C^{(n-1)}), \\ \Delta S &= S(C^{(n)}) - S(C^{(n-1)}), \\ \Delta g &= g(C^{(n)}) - g(C^{(n-1)}). \end{aligned}$$

Since the Monte Carlo moves are local (i.e. they involve only a small part of the RNA sequence) the computation of ΔE , ΔS and Δg is usually easier and faster than computing the full functions $E(C)$, $S(C)$ and $g(C)$.

We consider first Δg , and we provide an efficient algorithm for computing it. According to eq. (3.1), the genus is given by $g = (1 - \#V + \#E - \#F)/2 = (1 - L + (L + n_{arcs}) - n_{loops})/2$. Therefore:

$$\Delta g = \frac{1 + \Delta n_{arcs} - \Delta n_{loops}}{2}, \quad (5.5)$$

where

$$\Delta n_{arcs} = \begin{cases} -1 & \text{for a "remove the base-pair } i - j \text{" move,} \\ 1 & \text{for a "add the base pair } i - j \text{" move,} \\ 0 & \text{for a "shift or swap the base pair } i - j \text{" move.} \end{cases} \quad (5.6)$$

The difference Δn_{loops} can be computed by considering the loops containing the bases i and j . In principle there are 4 possible independent loops, two about i and two about j (see Figure 14). The connectivity of the RNA molecule can be such that the four loops are not independent. In Appendix A we describe an algorithm for computing the actual number of independent loops. Then it is sufficient to run the algorithm over $C^{(n)}$ and $C^{(n-1)}$ and compute the difference of loops, that is Δn_{loops} .

Secondly, the calculation of ΔE is more problematic. There is not yet an RNA energy model for any given topology. The most studied and well-defined model both from a theoretical and experimental point of view is for the spherical topology (i.e. genus= 0, that is RNA secondary structure without pseudoknots)[71]. The set of empirical ‘‘Turner’’ energy rules can be generalized in order to describe some simple class of pseudoknots [42] but the general case for *any* topology is still lacking. For ΔS the situation is slightly better, as one can model the configurational entropy of the RNA structure by using the theory of polymers (as already presented in [16] or [42]) and the inclusion of pseudoknots is in principle feasible. Therefore, in our numerical simulation we will use the ‘‘Turner’’ energy model, and even if this is not quite appropriate for higher topology, we expect the corrections to be small

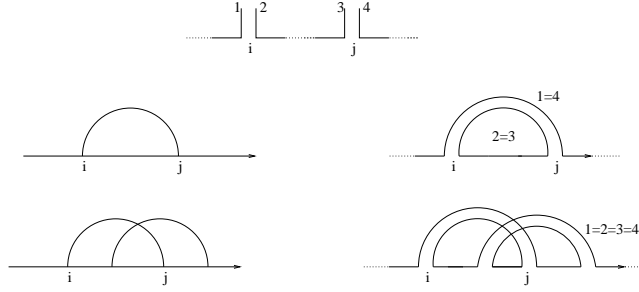


Figure 14: Two given bases i and j usually belong to 4 loops, when drawing the arc with the double-line notation. The loops are not always independent. Here there are two examples: a case with 2 independent loops (top), and a case with only one independent loop (bottom).

with respect to the over-all energy scale. We remind the reader that the purpose of this paper is to propose a new approach for the study of pseudoknots formation in RNA secondary structure. Thus at this point, it is reasonable to perform a preliminary analysis based on an approximate energy model. When a more complete energy model (including all the topologies) will be available, it will be sufficient to include it in the calculation of ΔE in our algorithm.

5.3 The “simulated annealing” method

One of the major problems about the Monte Carlo simulation of RNA folding, is that the energy landscape is usually very rough with metastable valleys separated by energy barriers which are “high” compared to the energy involved in each Monte Carlo move. This is a general situation in thermodynamic systems with many degrees of freedom (e.g. glasses, polymers, proteins etc.). where in addition to the global minimum energy configuration there may be many local minima separated by high energy barriers. The worst consequence is that the system can be trapped for a long time in such local minima and the Monte Carlo exploration of the energy landscape is no longer effective. In order to overcome this problem with RNA M.Schmitz and G. Steger in [9] proposed the use of a computational technique called “simulated annealing” method. It is a classical method which has been introduced for finding the minimum energy configuration of a system with a very rough energy landscape [72]. We briefly describe the algorithm:

- Step 1: generalize the partition function eq. (4.2) to the form:

$$\mathcal{Z}_{RNA} = \sum_{C_{ij}} e^{-\frac{1}{k_B\Theta}[E(C)-TS(T,C)+\mu g(C)]}, \quad (5.7)$$

and initialize $\Theta = \Theta_{max} > T$.

- Step 2: Starting from an initial configuration $C^{(0)}$ (e.g., the fully denaturated RNA configuration) sample n configurations by means of the Metropolis Monte Carlo method applied to eq. (5.7).
- Step 3: Go to Step 2, and replace Θ by a lower value, and $C^{(0)}$ by $C^{(n)}$. Repeat this step until the temperature of the system is equal to T . During the Monte Carlo process keep track all the time of the configuration with the lowest energy.

One can show that usually, the global minimum can be obtained by using a logarithmic rate [73]. In practice, other annealing schedules are possible: linear, hyperbolic, exponential, power-law schedules are often implemented.

Assuming that at low temperature an RNA molecule assumes a configuration which corresponds to the minimum energy, we can find such a configuration by using the simulated annealing method, starting the simulation with a value of Θ well above the melting temperature (say a few hundred degrees Celsius). A first check of this method is whether we can reproduce the results produced by deterministic algorithms such as “mfold” [55] or the “Vienna Package” [57]. For that purpose, it is sufficient to use the “Turner” energy model and run our algorithm with a large value of the chemical potential μ . Our preliminary tests showed that the minimum can be easily found for sequences with length up to around 300 bases. For longer RNA sequences, the simulation time increases and the minimum may be harder to find. In this cases we can use an additional feature of our model. In fact our approach offers also the interesting possibility of using the chemical potential for overcoming the energy barriers. It means that we can apply a “simulated annealing” method on μ rather than on T . Thus, starting with a low value of μ (where all the topologies with any genus are allowed) the Monte Carlo simulation can quickly explore regions which are very distant from each other in the energy landscape. Then by slowly increasing the value of μ we gradually constrain the simulation to select only planar configurations (i.e. secondary structures without pseudoknots), and the minimum energy configuration eventually. During this process, that is for intermediate values of μ , many configurations in thermal equilibrium are generated, and in general they correspond to diagrams with $\langle g \rangle \neq 0$, i.e. RNA configurations with pseudoknots. These configurations are the prediction of our algorithm and they should be compared with the experimental data. It is at this level that the value of μ can be tuned, in order to fit the data. The results of our preliminary investigations in this region of the phase diagram are very encouraging and promising. However, in this paper we limit ourselves to the description of this new method and of our algorithm. The results of our simulation will be published shortly.

6 Conclusions

In this paper we propose a new approach to the problem of RNA folding with pseudoknots. We start from a classifications of RNA pseudoknots based on their graphical representation by means of disk diagrams. A generic disk diagram is usually not planar, i.e. cannot be drawn on a plane surface without crossing lines. However, if the surface has a high enough genus (i.e. a sufficient number of “handles”), the diagram can always be drawn on that surface without any crossing. The precise correspondence is obtained by using a famous theorem by Euler, and it precisely corresponds to the topological classifications of RNA pseudoknots already introduced in [38]. Then we propose a statistical mechanics model where the formation of RNA pseudoknots is associated with fluctuations of the topology (eq. (4.2)). In order to do that we introduce a parameter, the topological “chemical potential”, which controls the rate of pseudoknots formation, and can be obtained by fitting experimental data. We then discuss the qualitative structure of the phase diagram for the RNA molecule in the plane $\{\mu, T\}$ and its interpretation. Finally we describe a Monte Carlo algorithm for the prediction of RNA pseudoknots. It is based on a standard Metropolis algorithm coupled to the “simulated annealing” method and we provide an explicit description of its implementation and use. A numerical investigation of this technique and the phase diagram is under way and will be published shortly.

Acknowledgments: We wish to thank the organizers of the EUROGRID meeting on “Random geometry: theory and applications” at Les Houches (France) on March 2004, where this work has been first presented. GV acknowledges the support of the European Fellowship MEIF-CT-2003-501547.

A An algorithm for computing n_{loops}

In this Appendix we describe an algorithm for computing the number of independent loops adjacent to the i -th and j -th nucleotides. It is useful for computing the variation of the genus when one of the Monte Carlo moves we described in Section 5. The algorithm we propose for counting the number of independent loops is based on tracking a walk along the diagram starting from the base i and marking the loop with an identifying number (or color). Namely, we represent the configuration C by means of the permutation involution σ_C (as described in Section 2), and the algorithm is:

```

START
v(1)=v(2)=v(3)=v(4)=0           % set the four flags to zero
pos=i                             % the start position is i-th base
color=1                            % using color 1
v(1)=color                         % mark the first flag with the color in use
do{                                 % start the first loop
    pos=sigma(pos)                 % follow the permutation involution
    if pos==i then v(2)=color      % check if it is either in i or j
    if pos==j then v(4)=color
    pos=shift(pos)                 % shift move (along the RNA circle)
    if pos==j then v(3)=color      % check if it is in i again
} while (position!=i)             % repeat until it returns at the starting point

if v(2)==0 then{                  % check if the second loop has been marked already
    color=color+1                  % if yes, change color
    pos=i                           % start again from i-th base
    v(2)=color                     % mark the second flag
    do{                             % repeat all the above for the second loop (at i)
        pos=shift(pos)
        if pos==j then v(3)=color
        pos=sigma(pos)
        if pos==j then v(4)=color
    } while (pos!=i)
}

if v(3)==0 then{                  % repeat all the above for the third loop (at j)
    color=color+1
    pos=j
    v(3)=color
    do{
        pos=sigma(pos)
        if pos==j then v(4)=color
        pos=shift(pos)
    } while (pos!=j)
}

if v(4)==0 then{                  % the fourth loop at j is independent from the
    color=color+1                  % previous ones if and only if it has not been
}                                  % marked yet

```

```

nloops=color          % the number of independent loops is the number
                      % of used colors
END

```

L is the length of the RNA sequence and the function `shift(pos)` is just the increment by 1 of the variable `pos` with period L , i.e. `shift(pos)=remainder(pos,L)+1`. At the end of the algorithm the variable “color” contains the number of independent loops n_{loops} . The algorithm runs in a time proportional to $O(L)$.

References

- [1] J. Couzin, “Breakthrough of the Year: Small RNAs Make Big Slash”, *Science* **298** (2002) 2296.
- [2] I. Tinoco Jr. and C. Bustamante, *J. Mol. Biol.* **293** (1999) 271.
- [3] P.A. Limbach, P.F. Crain and J.A. McCloskey, *Nucleic Acids Res.* **22** (1994) 2183.
- [4] U. Nagaswamy, N. Voss, Z. Zhang and G.E. Fox, *Nucleic Acids Res.* **28** (2000) 375.
- [5] A. Banerjee, J. Jaeger and D. Turner, *Biochemistry* **32** (1993) 153.
- [6] P. Brion and E. Westhof, *Ann. Rev. Biophys. Biomol. Struct.* **26** (1997) 113.
- [7] L. Laing and D. Draper, *J. Mol. Biol.* **237** (1994) 560.
- [8] M. Zuker and D. Sankoff, *Bull. Math. Biol.* **46** (1984) 591.
- [9] M. Schmitz and G. Steger, *J. Mol. Biol.* **255** (1996) 254.
- [10] R.R. Gutell, N. Larsen and C.R. Woese, *Microbiol Rev.* **58** (1994) 10.
- [11] C.R. Woese, R.R. Gutell, R. Gupta, H.F. Noeller, *Microbiol Rev.* **47** (1983) 621.
- [12] P.Higgs, *Phys. Rev. Lett* **76** (1996) 704.
- [13] R. Nussinov, G. Peickzenink, J. Griggs and D. Kleitman, *SIAM J. Appl. Math.* **35** (1978) 68.
- [14] C. Flamm, W. Fontana, L. Hofacker and P. Schuster, *RNA* **6** (2000) 325.
- [15] A.A. Mironov, L.P. Dyakonova and A.E. Kister, *J. Biomol. Struct. Dyn.* **2** (1985) 953.
- [16] H. Isambert and E.D. Siggia, *Proc. Natl. Acad. Sci. USA* **97** (2000), 6515.
- [17] A. Xayaphoummine, T. Bucher, F. Thalmann and H. Isambert, *Proc. Natl. Acad. Sci. USA* **100** (2003) 15310.
- [18] J.E. Tabaska, R.B. Cary, H.N. Gabow, G.D. Stormo, **14** (1998) 691.
- [19] M. Zuker, *Curr. Opin. Struct. Biol.* **10** (2000) 303.
- [20] C.W. Pleij, K. Rietveld and L. Bosch, *Nucleic Acids Res.* **13** (1985) 1717.
- [21] E. Westhof and L. Jaeger, *Current Opinion Struct. Biol.* **2** (1992) 327.

- [22] V.K. Misra and D.E. Draper, *Biopolymers* **48** (1998) 113.
- [23] J.P.D. Thirumalai, S.A. Woodson, *Proc. Natl. Acad. Sci. USA* **96** (1999) 6149.
- [24] V.K. Misra, R. Shiman and D.E. Draper, *Biopolymers* **69** (2003) 118.
- [25] M.S. Waterman, and T.H. Byers, *Mathematical Biosciences*, **77** (1985) 179.
- [26] A.L. Williams and I. Tinoco Jr., *Nucleic Acids Res.* **14** (1986) 299.
- [27] R. Nussinov and A.B. Jacobson, *PNAS* **77** (1980) 6309.
- [28] M. Zuker, *Science* **244** (1989) 48.
- [29] M. Zuker and P. Stiegler, *Nucleic Acids Res.* **9** (1981), 133.
- [30] I.L. Hofacker, W. Fontana, P.F. Stadler, S. Bonhoeffer, M. Tacker and P. Schuster, *Monatshefte f. Chemie* **125** (1994) 167.
- [31] S. Wuchty, W. Fontana, I.L. Hofacker, P. Schuster, *Biopolymers* **49** (1999) 145.
- [32] E. Rivas and S.R. Eddy, *J. Mol. Biol.* **285** (1999) 2053.
- [33] Y. Uemura, A. Hasegawa, S. Kobayashi and T. Yokomori, *Theoretical Computer Science* **210** (1999) 277.
- [34] T. Akutsu (2001), *Discr. Appl. Math.* **104** (2001) 45.
- [35] R.B. Lyngsø, C.N.S. Pedersen, *J. Comp. Biol.*, **7** (2000) 409.
- [36] R. Giegerich and J. Reeder, Technical Report 2003-03 (2003) University of Bielefeld.
- [37] J.S. Deogun, R. Donis, O. Komina and F. Ma, *Proc. Second Asia-Pacific Bioinformatics Conference (APBC2004)*, Dunedin, New Zealand CRPIT, 29. Chen, Y.P.P., Ed. ACS. 239-246.
- [38] H. Orland and A. Zee, *Nucl. Phys.* **B620** (2002) 456.
- [39] M. Pillsbury, H. Orland, A. Zee, <http://arXiv.org/physics/0207110>.
- [40] M. Pillsbury, J.A. Taylor, H. Orland and A. Zee, <http://arXiv.org/cond-mat/0310505>.
- [41] A.A. Mironov and V.F. Lebedev, *BioSystems* **30** (1993), 49.
- [42] A.P. Gulyaev, F.H.D. van Batenburg and C.W.A. Pleij, *RNA* **5** (1999) 609.
- [43] J.P. Abrahams, M. van den Berg, E. van Batenburg and C.W.A. Pleij, *Nucleic Acids Res.* **18** (1990), 3035.
- [44] A.P. Gulyaev, *Nucleic Acids Res.* **19** (1991), 2489.
- [45] I.L. Hofacker, in "Monte Carlo Approach to Biopolymers and Protein Folding", P. Grassberger, G. Barkema and W. Nadler (eds.), World Scientific, Singapore (1998), 171.
- [46] F. H. D. van Batenburg, A. P. Gulyaev and C. W. A. Pleij, *Nucleic Acids Res.* **29** (2001) 194.
- [47] F.H.D van Batenburg, A.P. Gulyaev and C.W.A. Pleij and J. Oliehoek, *Nucleic Acids Res.* **28** (2000) 201. The database is at <http://wwwbio.LeidenUniv.nl/~Batenburg/PKB.html>.

- [48] P. Hogeweg and B. Hesper, *Nucleic Acids Res.* **12** (1984) 67.
- [49] W. Fontana, A.M. Konings, P.F. Stadler and P. Schuster, *Biopolymers* **33** (1993) 1389.
- [50] H.H. Gan, S. Pasquali and T. Schlick, *Nucleic Acids Res.* **31** (2003) 2926.
- [51] T.C. Gluick and D.E. Drape, *J. Mol. Biol* **241** (1994) 246.
- [52] M.J. Serra, D.H. Turner and S.M. Freier, *Methods Enzymol.* **259** (1995) 243.
- [53] M. Zuker, D.H. Mathews and D.H. Turner, *RNA Biochemistry and Biotechnology*, J. Barciszewski and B.F.C. Clark, eds., NATO ASI Series (1999) Kluwer Academic Publishers.
- [54] J.S. McCaskill, *Biopolymers* **29** (1990) 1105.
- [55] M. Zuker, *Nucleic Acids Res.* **31** (2003) 3406.
- [56] D.H. Mathews, J. Sabina, M. Zuker and D.H. Turner, *J. Mol. Biol.* **288** (1999) 911.
- [57] I.L. Hofacker, *Nucleic Acids Res.* **31** (2003) 3429.
- [58] J. Ambjørn, M. Carfora, and A. Marzuoli, *The Geometry of Dynamical Triangulations*, Springer-Verlag, Berlin, 1998.
- [59] J. Ambjørn, B. Durhuus, T. Jonsson, *Quantum Geometry : A Statistical Field Theory Approach*, Cambridge University Press, 1997.
- [60] G. 't Hooft, *Nucl. Phys.* **B72** (1974) 461.
- [61] K. Binder and D.W. Heerman, *Monte Carlo Simulation in Statistical Physics*, Springer-Verlag, Berlin, 1992.
- [62] D. Frenkel and B. Smit, *Understanding Molecular Simulation*, 2nd edition, Academic Press, 2002.
- [63] I.L. Hofacker, P. Schuster, P.F. Stadler, *Discr. Appl. Math.* **88** (1998) 207.
- [64] N. Metropolis, A.W. Rosenbluth, M.N. Rosenbluth, A.H. Teller and E. Teller, *Jour. Chemical Physics* **21** (1953) 1087.
- [65] D.E. Knuth, *The Art of Computer Programming, Volume 3: Sorting and Searching*, 2nd ed. Reading, MA: Addison-Wesley, 1998.
- [66] D.E. Knuth, *The Art of Computer Programming, Volume 2: Seminumerical Algorithms*, 3rd ed. Reading, MA: Addison-Wesley, 1997.
- [67] W.H. Press, B.P. Flannery, S.A. Teukolsky, W.T. Vetterling, *Numerical Recipes in C : The Art of Scientific Computing*, Cambridge University Press, Cambridge, 1992.
- [68] C.J. Geyer, *Statist. Sci.* **7** (1992) 473.
- [69] J. Shao and D. Tu, *The Jackknife and Bootstrap*, Springer Verlag, 1995.
- [70] J.S. Liu, *Monte Carlo Strategies in Scientific Computing*, Chapter 2, Springer New York, 2001.
- [71] M. Zuker, *Methods Enzymol.* **180** (1989) 262.
- [72] S. Kirkpatrick, C.D. Gelatt and M.P. Vecchi, *Science* **220** (1983) 671.
- [73] S. Geman and D. Geman, *IEEE Trans. on Pattern Analysis and Machine Intelligence*, **6** (1984) 721.